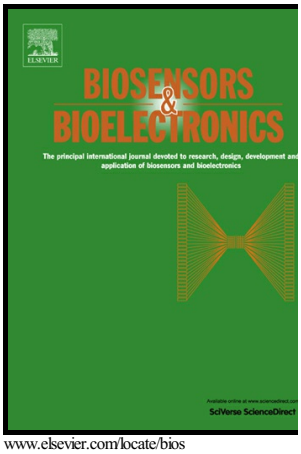

A ratiometric electrochemiluminescence detection for Cancer cells using g-C_3N_4 nanosheets and Ag-PAMAM-luminol nanocomposites

Yin-Zhu Wang, Nan Hao, Qiu-Mei Feng, Hai-Wei Shi, Jing-Juan Xu, Hong-Yuan Chen

www.elsevier.com/locate/bios

PII: S0956-5663(15)30382-1
DOI: http://dx.doi.org/10.1016/j.bios.2015.08.057
Reference: BIOS7953

To appear in: *Biosensors and Bioelectronic*

Received date: 13 July 2015
Revised date: 21 August 2015
Accepted date: 24 August 2015

Cite this article as: Yin-Zhu Wang, Nan Hao, Qiu-Mei Feng, Hai-Wei Shi, Jing-Juan Xu and Hong-Yuan Chen, A ratiometric electrochemiluminescence detection for Cancer cells using g-C_3N_4 nanosheets and Ag-PAMAM-luminol nanocomposites, *Biosensors and Bioelectronic* http://dx.doi.org/10.1016/j.bios.2015.08.057

A ratiometric electrochemiluminescence detection for cancer cells using g-C_3N_4 nanosheets and Ag-PAMAM-luminol nanocomposites

Yin-Zhu Wang, Nan Hao, Qiu-Mei Feng, Hai-Wei Shi, Jing-Juan Xu,*and Hong-Yuan Chen

State Key Laboratory of Analytical Chemistry for Life Science and Collaborative Innovation Center of Chemistry for Life Sciences, School of Chemistry and Chemical Engineering, Nanjing University, Nanjing 210093, P R China.

* Corresponding author. Tel. / Tax: +86-25-83597294.

E-mail: xujj@nju.edu.cn (J.-J. Xu).

Abstract

In this work, a dual-signaling electrochemiluminescence (ECL) ratiometric sensing approach for the detection of HL-60 cancer cells was reported for the first time. G-C_3N_4 nanosheets and Ag-PAMAM-luminol nanocomposits (Ag-PAMAM-luminol NCs) were prepared and served as reductive−oxidative and oxidative−reductive ECL emitters respectively. DNA probe functionalized Ag-PAMAM-luminol NCs would hybridize with aptamers modified onto magnetic beads. In the presence of HL-60 cells, the aptamer would conjugate with the target cell and release Ag-PAMAM-luminol NCs. After magnetic separation, released Ag-PAMAM-luminol NCs would hybridize with capture DNA on g-C_3N_4 nanosheets. ECL from g-C_3N_4 nanosheets coated on ITO electrode at −1.25 V (vs SCE) could be quenched by Ag-PAMAM-luminol NCs due to the resonance energy transfer (RET) from g-C_3N_4 nanosheets to Ag NPs. Meanwhile, Ag-PAMAM-luminol brought the ECL signal of luminol at +0.45 V (vs SCE). Thus, the concentration of HL-60 cancer cells could be quantified by both the quenching of ECL from g-C_3N_4 nanosheets and the enhancement of ECL from luminol. By measuring the ratio of ECL intensities at two excitation potentials, this approach could achieve sensitive and reliable detection for cancer cells in a wide range from 200 cells/mL to 9000 cells/mL with the detection limit of 150 cells(S/N=3).

Keywords: Electrochemiluminescence, Ratiometric, Biosensor, G-C_3N_4, Luminol, HL-60 cancer cells

1. Introduction

Pioneered by Hercules and Lytle's research group, electrochemiluminescence (ECL) has been introduced as a promising chemiluminescence method in analytical applications because of its low background, high sensitivity, good temporal/spatial control and wide dynamic range(Zhou et al. 2015). This analytical technique has attracted considerable attention in DNA detection, immunoassay and cancer screening(Gu et al. 2015). However, false positive or negative errors are inevitable when the detection was based on one signal change because of the instrumental or some environmental factors(Li et al. 2012). To eliminate these interferences and make the detection more convincing, we have successfully developed the first ECL ratiometric biosensor based on the large absorption cross section and catalytic ability of luminol-modified Pt NPs(Zhang et al. 2013a). On this basis, we also studied a highly sensitive microRNA ratiometric ECL sensor that employed enzyme-assisted signal amplification and distance dependent resonance energy transfer(Hao et al. 2014).

These two sensors are all constructed on the synergistic effect of traditional ECL active materials, CdS nanocyrstals and luminol modified metal nanoparticles. Although Cd-based semiconductor nanocyrstals, such as CdS(Zhang et al. 2012), CdSe(Huang et al. 2015) and CdTe(Liang et al. 2014), had been extensively used in ECL detections because of superior performances, their application fields are severely limited because of the potential toxicity both to health and environment. Among ECL luminescence reagents, luminol and its derivatives are another kinds of well known

and widely applied ECL emitters due to their high luminous efficiency and good stability(Jiang et al. 2015). Metal nanoparticles can effectively catalyze the oxidation of luminol and enhance the ECL emission. But the loading volume of luminol molecules on nanoparticles isn't satisfying and sometimes the ECL signal isn't strong enough. Exploring the feasibility of ECL active nano-materials in ratiometric sensing system is necessary for expanding the application fields.

Recently, growing attentions have been concentrated on graphite-like carbon nitride materials. G-C_3N_4 is a kind of metal-free semiconductor nanoparticles with p-conjugated graphitic planes formed by the sp^2 hybridization of carbon and nitrogen, which is chemical and thermal stable with medium band gap(Zhang et al. 2013b). Besides the excellent catalytic, optical and electronic properties, researchers also have investigated the ECL behaviors of g-C_3N_4, demonstrating that g-C_3N_4 may be a new class of efficient and promising luminophore for ECL sensing(Cheng et al. 2012). Like other semiconductor nanocrystals(Shan et al. 2009), the ECL emission from g-C_3N_4 also could be quenched by noble metal nanoparticles when the spectra overlap existed. PAMAM dendrimers are highly branched three-dimensional macromolecules with hydrophilic terminal functional amino-groups (-NH_2)(Satija et al. 2011). The unique space structures make them excellent candidates for immobilizing molecules or nanoparticles(Han et al. 2010). Therefore, PAMAM nanocomposites can load high volume of luminol molecules and metal nanoparticles to effectively quench the ECL signal of g-C_3N_4 nanosheets (NSs) and bring enhanced luminol emission.

In this work, we introduced two novel materials, Ag-polyamidoamine

(PAMAM)-luminol nanocomposites and graphite-like carbon nitride (g-C_3N_4) into ECL ratiometric sensing system and successfully built ECL ratiometric cell sensor for the first time. Scheme 1 illustrates the principle of this dual-signaling ECL biosensor towards cancer cells. First, we prepared the Ag-PAMAM-luminol nanocomposites (NCs) (scheme A). After functionalized with Probe DNA (pDNA) and bio-bar-code DNA (bbcDNA), the prepared composite pDNA-Ag-PAMAM was added to hybridize with the aptamer on magnetic microbeads (MBs). After adding various numbers of HL-60 cells, the aptamer combined with the glycoprotein at cell surface and released pDNA-Ag-PAMAM. G-C_3N_4 was immobilized on the electrode surface and functionalized with capture DNA. Then the released Ag-PAMAM-luminol NCs were added to hybridize with the complementary DNA and immobilized on the electrode (scheme B). The increase of cell concentrations resulted in the increase of the pDNA-Ag-PAMAM bioconjugate on the electrode. The ECL signal of g-C_3N_4 NSs decreased while the ECL intensity of luminol markedly increased in the presence of common coreactant H_2O_2. The ratio change of the two signals is corresponding to the change of the cell concentrations in a wide range from 200 cells/mL to 9000 cells/mL with the detection limit of 150 cells/mL.

Scheme 1

2. Experimental Section

2.1. Reagents and material

Indium-tinoxide (ITO)-coated (thickness: 100 nm; resistance: 10 Ωsqr^{-1}) aluminosilicate glass slides were obtained from China Southern Glass (Shenzhen,

China). Melamine was obtained from Fuchen Chemical Reagent Co. (Tianjin, China). $AgNO_3$ was purchased from Shanghai Shenbo Chemical Reagent Co., LTD. $NaBH_4$ was purchased from Tianjin Chemical Reagent Institute. H_2SO_4 was supplied by Shanghai Chemical Reagent Co. Ltd., China. Luminol (98%), PAMAM dendrimer (ethylenediamine core, generation 4.0, 10 wt% in methanol, 64 surface primary amino groups), glutaraldehyde(GA), bovine serum albumin (BSA, 96-99%), N-hydroxy succinimide (NHS) and 1-ethyl-3-(3-dimethylaminopropyl) carbodiimide hydrochloride (EDC), chitosan (CS) were purchased from Sigma-Aldrich Co. (St. Louis, MO, USA). Complementary DNA, probe DNA and bio-bar-code DNA were purchased from Shenggong Bioengineering Ltd. Company (Shanghai, China), and the sequences are listed in Table 1. Magnetic beads (20 nm) were purchased from Xi'an GoldMag Nanobiotech Co., Ltd. Phosphate buffered solution (PBS, pH 7.4) (0.1 M) was prepared by mixing standard stock solutions of KH_2PO_4 (0.1 M), K_2HPO_4 (0.1 M), KCl (0.1 M), and 3 mM NaCl. Millipore ultrapure water (specific resistance of 18 MΩ cm) was used throughout this study.

HL-60 cells were cultured in DMEM medium supplemented with 10% fetal calf serum, and the cells were maintained at 37 °C in a humidified atmosphere (95% air and 5% CO_2). Cells were collected in the exponential phase of growth and washed twice with ice-cold sterile PBS.

Table 1.

2.2. Apparatus

The preparation of g-C_3N_4 NSs was carried out in a tube furnace (GSL 1400X, Kejing

Materials Technology Lt. Co., Hefei, China). Transmission electron micrographs (TEM) were obtained on JEM-1011 and JEM-2100 transmission electron microscope (JEOL Ltd., Japan). Fourier-transformation infrared (FTIR) spectra were performed on an IR-Prestige-21 FTIR spectrometer (Shimadzu Co., Japan). X-Ray nanoparticle diffraction (XRD) patterns were measured with a Japan Rigaku D/max-3C using Cu Karadiation. To investigate the optical properties of the g-C_3N_4 aqueous solution. UV-vis absorption spectra were recorded using a UV-vis spectrophotometer (Nanodrop-2000C, Nanodrop, USA). MPI-A ECL analyzer (Xi'an Remax Electronic Science & Technology Co. Ltd., Xi'an, China) was used to monitor the ECL emissions. ECL detection experiments were performed with a conventional three-electrode system containing a platinum wire as counter electrode, a saturated calomel electrode (SCE) as reference electrode and the modified ITO electrode as working electrode.

2.3 Synthesis of g-C_3N_4 NSs and preparation of g-C_3N_4 aqueous solution

g-C_3N_4 NSs were prepared following the previously published method with some slight modifications(Chi et al. 2012). Briefly, 5.0 g white melamine powder was placed into an alumina crucible and heated at 550 °C for 4 h in a muffle furnace with a ramp of about 3 °C/min and kept at this temperature for another 4 h in air. After naturally cooling to room temperature, the yellow bulk g-C_3N_4 product was ground to powder for further use. Then, 0.02 g g-C_3N_4 powder was dispersed in 100 mL water, after addition of 0.1 g H_2SO_4 (5 M), the mixture was sonicated for 30 s, which was further heated in a 70 °C under stirring until it turned into a transparent solution, then cooled it down and stored at room temperature.

2.4 Preparation of g-C_3N_4-CS/complementary DNA modified electrode

Before preparing the ECL sensing interfaces, a sheet of ITO glass (20 mm×8 mm) was thoroughly ultrasonically cleaned sequentially with acetone, ethanol and water, successively. Then the ITO slices were boiled in 2 M KOH dissolved in isopropyl alcohol for 15 min and dried at 120 °C. A section of plastic transparent tape was punched with a hole (6 mm diameter) and then attached on the conductive surface of ITO glass to provide an effective working surface area for the electrochemical measurements. Meanwhile, 0.5 mL g-C_3N_4 suspension (0.015 mg mL^{-1}) was dispersed in 0.5 mL 0.3% CS solution (in 0.1 M acetic acid) to obtain a homogeneous g-C_3N_4-CS suspension with sonication. Then 30 μL g-C_3N_4-CS suspension was dropped on the cleaned substrates and dried at 4 °C. After that, 30 μL EDC (20 mg) and NHS (10 mg) were added onto the electrode and incubated for 2 h at 37 °C. Afterwards, 500 μL complementary DNA (10^{-6} M) was added onto the electrode and the mixture was incubated at 37 °C over night. Finally the medium was removed and 3 μL BSA (1 wt%) solution was added for 1 h to block nonspecific binding sites. The prepared electrode was stored at 4 °C until use.

2.5 Preparation of Ag-luminol NCs; Ag-PAMAM NCs and Ag-PAMAM-luminol NCs

Ag-luminol NCs were prepared according to the following method: 200 μL EDC (20 mg) and NHS (10 mg) was added onto 1.0 mL carboxyl group of Ag colloidal solution (Lv et al. 2014) and incubation for 2 h at 37 °C, then added 1.0 mL of luminol (10^{-3} M), continued to incubate for an hour to synthetic the Ag-luminol NCs. The PAMAM dendrimer-encapsulated silver nanocomposites (Ag-PAMAM NCs)

were prepared by using an in situ synthesis method with the chemical reduction of the $AgNO_3$-PAMAM hybrid in the presence of $NaBH_4$. Briefly, 4×10^{-5} mol of PAMAM dendrimers containing 64 surface amino groups was initially dissolved in 10 mL of methanol, and then the hybrid was adequately stirred. Following that, 1.0 mL of $AgNO_3$ methanol solution (0.1 M) was injected into 10 mL of the PAMAM dendrimer solution. The resultant hybrid was stirred at 4 °C under nitrogen for 1 h. During this process, Ag^+ ions were immobilized by the coordinative bonding to the amino groups of the dendrimer. Afterwards, the Ag-PAMAM NCs were synthesized by slow addition of 20-fold excess of 0.5 M $NaBH_4$ dissolved in distilled water under stirring. After 30 min, the Ag-PAMAM suspension was dialyzed with a cellulose dialysis sack having a molecular weight cutoff of 12000 to remove impurities. Finally, the collected products of solid state were washed for three times by ethanol and doubly distilled water, respectively. 1.0 mg of Ag-PAMAM NCs was redispersed in 1.0 mL water for further use. Finally, the Ag-PAMAM NCs was dispersed in 1.0 mL doubly distilled water containing glutaraldehyde (3 mM), which as crosslinking agent to connect the end amino groups of PAMAM and luminol with amino groups. After activating the amino groups of PAMAM for 2 h, 500 μL, pH 7.4 luminol (0.025 M) was added to the mixture solution for another 2 h reaction in darkness.

2.6 Preparation of pDNA-Ag-luminol bioconjugates; pDNA-Ag-PAMAM bioconjugates and pDNA-Ag-PAMAM-luminol bioconjugates

The pDNA and bbc DNA (bio bar code) modified with a thiol at their 5'-end were used to prepare these bioconjugates. Briefly, 50 μL pDNA (1 μM) and 500 μL bbc

DNA (10 μM) were activated with 2 μL of 10 mM TCEP before use in order to reduce disulfide bonds. 50 μL pDNA (1 μM) and 500 μL bbc DNA (10 μM) were then added to 100 μL Ag-luminol; Ag-PAMAM; and Ag-PAMAM-luminol solution and stirred at 37 °C overnight separately. Afterward, 0.1 mL PBS solution containing 3.0 M NaCl was added to the mixture stepwise for stabilizing the obtained probe, which was centrifuged and washed with PBS three times, finally resuspensed in1.0 mL PBS.

2.7. Preparation of g-C_3N_4/PAMAM modified electrode; g-C_3N_4/Ag-luminol modified electrode; Ag-PAMAM/g-C_3N_4 electrode and Ag-PAMAM-luminol/g-C_3N_4 electrode

30 μL EDC (20 mg) and NHS (10 mg) were added onto the g-C_3N_4-CS modified electrode and incubated for 2 h at 37 °C, then 30 μL PAMAM (5×10^{-5}) was dropped on the electrode and incubated for another 2 h to form g-C_3N_4/PAMAM modified electrode. Similarly, the other three types of electrode preparation according to the following method: 30 μL EDC (20 mg) and NHS (10 mg) were added onto the g-C_3N_4-CS/complementary DNA modified electrode and incubated for 2 h at 37 °C. Afterwards, 30 μL pDNA-Ag-luminol bioconjugates (g-C_3N_4/Ag-luminol modified electrode) or 30 μL pDNA-Ag-PAMAM bioconjugates (g-C_3N_4/Ag-PAMAM modified electrode) or 30 μL pDNA-Ag-PAMAM-luminol bioconjugates (g-C_3N_4/Ag-PAMAM-luminol modified electrode) was added onto the electrode and the mixture was incubated at 37 °C over night.

2.8. Fabrication of the ECL biosensor

Firstly, 100 μL carboxylated magnetic microbeads (MBs) were transferred into a 1.5 mL Eppendorf tube and were washed three times with 500 μL PBS buffer, then, MBs

were resuspended in pH 7.4 PBS buffer. Secondly, 100 μL EDC (0.2 M) and NHS (0.1 M) were added to the EP tube, and the mixture was incubated at 37 °C for 1 h to activate the carboxyl groups on the MBs. After being washed with 0.1 M PBS buffer (pH 7.4), 200 μL thiol-modified aptamer (1.0×10^{-6} M) was added. Thiol-modified aptamer was activated with TCEP (10 mM) for 1 h before attaching to MBs. After shaking gently for 16 h at room temperature, the aptamer-MBs biocomposite was "aged" in the solution (0.3 M NaCl, 10 mM Tris-acetate, pH 7.4) for another 24 h. Excess reagents were removed by magnetic force, followed by adding 500 μL of the above pDNA-Ag-PAMAM-luminol solution and incubating for 2 h at 37 °C to obtain the MB-probe biocomposite. Finally, the MB-probe biocomposite was incubated with 100 μL of PBS containing different numbers of HL-60 cells at room temperature for 50 min and the pDNA-Ag-PAMAM-luminol bioconjugate released from the MB-probe biocomposite was separated from the solution with a magnetic field.

2.9. ECL detection

After the above reactions and magnetic separation, the g-C_3N_4-CS/complementary DNA/electrode was immersed in the released pDNA-Ag-PAMAM -luminol solution at 37 °C for 1 h, and washed thoroughly with doubly distilled water. Then the ECL measurements were performed, the resultant pDNA-Ag-PAMAM -luminol modified electrode was performed in a detector cell containing 0.1 M PBS (pH 7.4) solution with 10 mM H_2O_2 and 0.1 M KCl at room temperature. The voltage of the photomultiplier tube (PMT) set at -400 V and the potential scan from -1.3 V to 0.6 V (vs. SCE) with a scan rate of 100 mV s^{-1} in the process of detection.

3 Results and discussion

3.1 Characterization of g-C_3N_4 NSs

G-C_3N_4, as the sensing layer of this cytosensor, has a significant impact on the detection of cancer cells. Fig.1A displayed the TEM image of g-C_3N_4 NSs. A wrinkled-layer structure with several stacking layers could be clearly observed in the g-C_3N_4 sample with an average size less than 100 nm. It is worth mentioning that the dispersion can be very stable for several months without any precipitates.

Fig.1B showed the FT-IR spectra of g-C_3N_4 NSs. The peak at 807 cm^{-1} was assigned to the vibration of the tri-s-triazine (Ou et al. 2015). The absorption bands located at 1180 cm^{-1} and 1239 cm^{-1} were corresponding to either triangular C−N(−C)−C or bridging C−NH−C units survived after thermal oxidation etching in the layers of nanosheets. The absorption bands at 1386 cm^{-1} and 1543cm^{-1} were corresponding to N−H bending/C−N stretching, respectively, and a peak of 1728 $cm^{-1}$was attributed to C=O stretching. The broad peak at 3176 cm^{-1} was corresponding to N-H stretching. All these indicating the successful functionalization of carboxyl group on g-C_3N_4 NSs. (Chen et al. 2014; Lu et al. 2014).

The XRD patterns of g-C_3N_4 NSs was presented in Fig. 1C. The strong peak at 27.6° was the characteristic of the stacking peak of pi-conjugated layers and indexed to the (002) plane of graphitic materials. The peak at 13.12° was indexed to the (100) plane of g-C_3N_4 NSs and assigned to an in-plane structural packing motif. The much weaker peak for the exfoliated products implied a decreased planar size of the layers (Li et al. 2014).

Fig. 1D showed the UV-vis absorption (black line) and ECL spectrum emission (red line) spectra of the aqueous dispersion of g-C_3N_4 NSs. The dispersion showed an absorption peak at 296 nm and a strong ECL emission peak centered at about 440 nm, which was consistent with the previous literatures (Cheng et al. 2012; Deng et al.).

Fig. 1.

3.2 Characteristics of Ag NPs and Ag-PAMAM-luminol NCs by TEM and UV-vis

As shown in Fig. 2A, the Ag NPs were well dispersed with the average diameter of about 9 nm. It's worth noting that no aggregation of Ag NPs was found after 2 months of preservation at the room temperature. The TEM image for Ag-PAMAM NCs was shown in Fig. 2B. Due to the poor electrical conductivity of PAMAM, the TEM image of Ag-PAMAM NCs was vaguer than that of Ag NPs. After adding luminol molecules into the colloid, the TEM image showed an obvious aggregation, but the dimension of single Ag nanoparticle changed little (Fig.2C).

UV-vis absorption spectra analysis provide more effective information on the successful immobilization of luminol onto the Ag-PAMAM NCs. As shown in Fig. 2D, luminol (curve a) had two absorption peaks at 293 nm and 340 nm, and Ag (curve b) had a maximum absorption peak at about 420 nm. The UV-vis spectrum of Ag-PAMAM-luminol NCs presents the characteristic peaks of luminol at 300 nm and 360 nm and the Ag absorption peak at about 440 nm, indicating that we successfully synthesized Ag-PAMAM-luminol nanocomposite. Moreover, the absorption spectrum of Ag-PAMAM-luminol at about 440 nm is well overlapped with the ECL spectrum of g-C_3N_4, suggesting that Ag NPs in the composite could quench the ECL of g-C_3N_4.

Fig. 2.

3.3. Comparison of ECL responses by using various modified electrodes

To elucidate the feasibility of the developed electrochemical biosensor using pDNA-Ag-PAMAM-luminol bioconjugates, a comparative study was carried out with different modified electrodes in pH 7.4 PBS containing 10 mM H_2O_2 with the same assay protocol. The comparison was evaluated on the basis of the change in the ECL intensity with no analytes. As can be seen from Fig. 3, one large ECL peak at the potential of -1.28 V (curve a) appeared when the potential was scanned in the negative direction from -1.3 V to 0.6 V. Upon the potential scan with an initial negative direction, the g-C_3N_4-CS immobilized on the electrode was reduced to g-$C_3N_4^{\cdot -}$. Meanwhile, the coreactant H_2O_2 was reduced to the strong oxidant $^{\cdot}OH$, then $^{\cdot}OH$ could react with g-$C_3N_4^{\cdot -}$ to produce the excited states of g-$C_3N_4^{*}$, which decayed to the ground state with light emitting (Chi et al. 2012). The possible ECL mechanism of g-C_3N_4 is as follows:

$$g\text{-}C_3N_4 + e^- \rightarrow g\text{-}C_3N_4^{\cdot -} \quad (1)$$

$$H_2O_2 + e^- \rightarrow OH^- + {}^{\cdot}OH \quad (2)$$

$$^{\cdot}OH + g\text{-}C_3N_4^{\cdot -} \rightarrow g\text{-}C_3N_4^{*} + OH^- \quad (3)$$

$$g\text{-}C_3N_4^{*} \rightarrow g\text{-}C_3N_4 + h\nu \quad (4)$$

After PAMAM was modified on the g-C_3N_4 electrode by the reaction between amino groups on the surface of PAMAM and carboxyl groups on the surface of the g-C_3N_4, ECL intensity weakened slightly due to the poor electroconductivity of PAMAM (curve b). To achieve ratiometric sensing, we firstly adopted similar approaches

applied in previous works that modified luminol molecules onto metal NPs by preparing Ag-luminol NCs (Zhang et al. 2014). After Ag-luminol NCs functionalized with pDNA hybridized with g-C_3N_4-cDNA, the ECL peak appeared at about -1.28 V obviously decreased (curve c) due to the RET between g-C_3N_4 and Ag NPs and another weak ECL peak can be observed at about 0.5 V, which was corresponding to the emission from luminol(Wang et al. 2015). In order to further weaken the signal of g-C_3N_4 and enhance the signal of luminol, we used PAMAM to carry more Ag NPs and luminol. When Ag NPs was encapsulated by PAMAM and immobilized onto the electrode, ECL intensity at -1.28 V decreased 5.8 folds compared with the pDNA-Ag-luminol/g-C_3N_4-CS modified electrode (curve d). It is most likely a consequence of the fact that PAMAM could encapsulated a lot of silver nanoparticles. When the complementary DNA/g-C_3N_4-CS modified electrode was incubated with pDNA-Ag-PAMAM-luminol bioconjugates, the ECL intensity of luminol increased 4.2 folds (curve e) compared with the pDNA-Ag-luminol/g-C_3N_4-CS modified electrode (curve c), indicating that Ag-PAMAM could packaged a large number of luminol. Meanwhile, the ECL peak at about -1.28 V further decreased compared with curve c. This phenomenon could be attributed to the higher energy transfer efficiency, which caused by the increased spectral overlap degree. Changes of UV-vis absorption spectra of Ag-PAMAM NCs (Fig. 2.D curve b) and Ag-PAMAM-luminol NCs which afterwards modifying with luminol (Fig. 2.D curve c) could be seen from Fig. 2.D. The red shift of the peak from around 420 nm to 450 nm expanded the spectra overlap range between the absorption spectrum of Ag NPs and the ECL spectrum of g-C_3N_4

nanosheets. Thus Ag-PAMAM-luminol NCs had a better quenching effect than Ag-PAMAM NCs. In addition, the pDNA with a 33-bases and 45-bases were used to investigate the distance dependence of the ECL-RET efficiency. In the presence of 1.0 μM cDNA and Ag-PAMAM-luminol NPs, the distances between two emitters were about 11, and 15 nm, respectively. The ECL quenching efficiency was 88.4%, and 52.54%, respectively, which means that the higher quenching efficiency was obtained at shorter separation distance. This is due to the energy transfer efficiency inversely linked to separation distance of the donor and acceptor.

Fig. 3.

3.4. ECL detection of Cancer Cells

Before the application of this sensor to the accurate analysis, several experimental parameters such as the amount of g-C_3N_4 NSs, the concentration of H_2O_2, the ratio of the concentration of luminol to Ag-PAMAM, and the ratio of the concentration of pDNA to Ag-PAMAM-luminol were investigated in detail (Fig. S1). The analytical performance of designed method was characterized by determining the number of HL-60 cancer cells under these optimal experimental conditions. As shown in Fig 4A, the ECL intensity of g-C_3N_4 decreased and the ECL peak of luminol increased correspondingly when the number of HL-60 cancer cells increased from 0 to 11000. Fig. 4B indicated the relationship between HL-60 concentration and ECL intensities from g-C_3N_4 and luminol respectively. The logarithmic value of $ECL_{g\text{-}C_3N_4}/ECL_{luminol}$ linearly depended on the logarithm of the number of HL-60 cancer cells in the range

of 200 to 9000 cells/mL with a correlation coefficient of 0.9957 (Fig 4C). The linear regression equation was log ($ECL_{g\text{-}C_3N_4}/ECL_{luminol}$)=-2.5×$10^{-4}$log[C]+1.526. The detection limit corresponding to a signal-to-noise ratio of 3 was 150 cells/mL.

Fig. 4.

3.5. Selectivity of the ECL biosensor

To explore the selectivity of this sensor over HL-60 cancer cells, some contrast experiments were performed on Hela cells, PC-12 cells, K562 cells, HL-60 cells, and MCF cells with the same concentration of 4000 cells/mL or without any cancer cells (Fig. 4D). Obviously, compared with the blank solution, almost no signal changes were acquired from the Hela cells, PC-12 cells, K562 cells and MCF cells. The ECL intensity decreased substantially only in the presence of HL-60 cells. We also explored the stability (Fig. S2) and reproducibility of this sensor. The reproducibility of sensor system has been evaluated by five repeated measurement of detecting 4000 cells/mL HL-60 cancer cells and the relative standard deviations (R.S.D.) of the assay for six detections using six freshly prepared modified electrodes was about 4.9%, indicating that the reproducibility of the proposed biosensor for determining HL-60 cancer cells was acceptable. These results indicated that our biosensor exhibited good selectivity for the assay of target HL-60 cells over Hela cells, PC-12 cells, K562 cells and MCF cells while displayed a good stability and reproducibility.

4. Conclusions

In summary, a novel ECL biosensor for HL-60 cancer cell detection was successfully developed based on the application of g-C_3N_4 nanosheets and Ag-PAMAM-luminol

nanocomposits. In the presence of target cells, reductive-oxidative ECL emission from g-C_3N_4 nanosheets could be quenched by Ag-PAMAM-luminol NCs due to the spectra overlap between the absorption spectrum of Ag NPs and the ECL spectrum of g-C_3N_4 nanosheets while luminol brought the oxidative-reductive ECL emission at the same time. The concentration of target cells could be quantified by the ratio of ECL intensities at two excitation potentials with a detection limit as low as 150 HL-60 cells. In addition, the sensor has high selectivity and good linear range. These results indicate that the developed ECL biosensor can be used to detect HL-60 cells effectively.

Acknowledgements

We appreciate the financial support of this project from the 973 Program (Grant 2012CB932600), National Natural Science Foundation of China (No. 21475058, 21535003) and the Science and technology support project (BE2013073) of Jiangsu Province, China. This work was also supported by a Project Funded by the Priority Academic Program Development of Jiangsu Higher Education Institutions.

References

Chen, H., Tan, X., Zhang, J., Lu, Q., Ou, X., Ruo, Y., Chen, S., 2014. RSC Adv. 4, 61759-61766.

Cheng, C.M., Huang, Y., Tian, X.Q., Zheng, B.Z., Li, Y., Yuan, H.Y., 2012. Anal. Chem. 84, 4754-4759.

Chi, Y., Chen, L., Huang, D., Ren, S., Dong, T., Chen, G.N., 2012. Nanoscale,

225-230.

Deng, S.Y., Yuan, P.X., Ji, X.B., Shan, D., Zhang, X.J., 2014. ACS Appl. Mater. Interfaces 7, 543-552.

Gu, W., Deng, X., Gu, X., Jia, X., Lou, B., Zhang, X., Li, J., Wang, E., 2015. Anal Chem. 87, 1876-1881.

Han, H.J., Kannan, R.M., Wang, S., Mao, G., Kusanovic, J.P., Romero, R., 2010. Adv. Funct. Mater. 20, 409-421.

Hao, N., Li, X.L., Zhang, H.R., Xu, J.J., Chen, H.Y., 2014. Chem. Commun. 50, 14828-14830.

Huang, T., Meng, Q., Jie, G., 2015. Biosens. Bioelectron. 66, 84-88.

Jiang, X., Wang, H., Yuan, R., Chai, Y., 2015. Biosens. Bioelectron. 63, 33-38.

Li, N., Chang, C., Pan, W., Tang, B., 2012. Angew. Chem. Int. Ed. 51, 7426-7430.

Li, X., Zhang, X., Ma, H., Wu, D., Zhang, Y., Du, B., Wei, Q., 2014. Biosens. Bioelectron. 55, 330-336.

Liang, H., Song, D., Gong, J., 2014. Biosens. Bioelectron. 53, 363-369.

Lu, Q., Zhang, J., Liu, X., Wu, Y., Yuan, R., Chen, S., 2014. Analyst 139, 6556-6562.

Lv, X., Li, Y., Cao, W., Yan, T., Li, Y., Du, B., Wei, Q., 2014. Sens. Actuators, B. 202, 53-59.

Ou, X., Tan, X., Liu, X., Lu, Q., Chen, S., Wei, S., 2015. Biosens. Bioelectron. 70, 89-97.

Satija, J., Sai, V.V.R., Mukherji, S., 2011. J. Mater. Chem. 21, 14367-14367.

Shan, Y., Xu, J.J., Chen, H.Y., 2009. Chem. Commun. 905-907.

Wang, J.X., Zhuo, Y., Zhou, Y., Yuan, R., Chai, Y.Q., 2015. Biosens. Bioelectron. 71, 407-413.

Zhang, H.R., Wu, M.S., Xu, J.J., Chen, H.Y., 2014. Anal. Chem. 86, 3834-3840.

Zhang, H.R., Xia, X.H., Xu, J.J., Chen, H.Y., 2012. Electrochem. Commun. 25, 112-115.

Zhang, H.R., Xu, J.J., Chen, H.Y., 2013a. Anal. Chem. 85, 5321-535.

Zhang, X., Xie, X., Wang, H., Zhang, J., Pan, B., Xie, Y., 2013b. J. Am. Chem. Soc. 135, 18-21.

Zhou, H., Yue, H., Zhou, Y., Wang, L., Fu, Z., 2015. Sens. Actuators, B. 209, 744-750.

Figure Captions

Scheme 1. Schematic illustration of the ratiometric electrochemiluminescence sensing system for HL-60 cancer cells detection.

Fig. 1. (A) TEM image of g-C_3N_4 NSs; (B) FT-IR spectra of g-C_3N_4 NSs; (C) XRD patterns of g-C_3N_4 NSs; (D) ECL spectrum of g-C_3N_4 on ITO electrode.

Fig. 2. (A) TEM image of Ag NPs; (B) Ag-PAMAM NCs; (C) Ag-PAMAM-luminol NCs; (D) The UV-vis absorption spectra of (a)luminol, (b) Ag-PAMAM NCs, (c) Ag-PAMAM-luminol NCs.

Fig. 3. Cyclic ECL on potential curves in various cases. (a) g-C_3N_4 electrode; (b) PAMAM/g-C_3N_4 electrode; (c) Ag-luminol/g-C_3N_4 electrode; (d) Ag-PAMAM/g-C_3N_4 electrode; (e) Ag-PAMAM-luminol/g-C_3N_4 electrode; ECL detection buffer:0.1 M PBS (pH 7.4) containing 10 mM H_2O_2. PMT was set at 400 V. Scan range: -1.3 to 0.6 V. Scan rate: 0.1 V/s.

Fig. 4. (A) Cyclic ECL curves at the dual-signaling ECL sensing interface with different number of HL-60 cancer cells: 0, 500, 2000, 3000, 4000, 5000, 6000, 9000, 11000 cells/mL from a to i, respectively. The left signal was induced by g-C_3N_4, and the right signal was induced by luminol. (B) Relationship between the ECL intensity of (a) g-C_3N_4 NSs or (b) luminol and the number of HL-60 cancer cells. (C) Relationship between the lg($ECL_{g\text{-}C3N4}$/$ECL_{luminol}$) and the number of HL-60 cancer cells. (D) Bar graph of the ECLg-C_3N_4/$ECL_{luminol}$ in the presence of different kinds of 4000 cells/mL cancer cells and without cell. The ECL detection conditions same as in Fig. 3.

Table 1. DNA Sequences used in this Work

Name	Sequences (5′ to 3′)
HL-60 Cell Aptamer	5'-NH_2-TTT ATC CAG AGT GAC GCA GCA TGCCCTAGT TAC TAC TAC TCT TTT TAG CAA ACG CCC TCG CTT TGG ACA CGG TGG CTT AGT-3'
c DNA	5'-NH_2- ATC CAG AGT GAC GCA GCA TGC CCT AGT TAC TAC TAC TCT TTT-3'
p DNA	5'-SH-GTA GTA ACT AGG GCA TGC TGC GTC ACT CTG GAT-3'
bbc DNA	5'- SH-ACG CTA GCT ATG CTT-3'

Scheme 1.

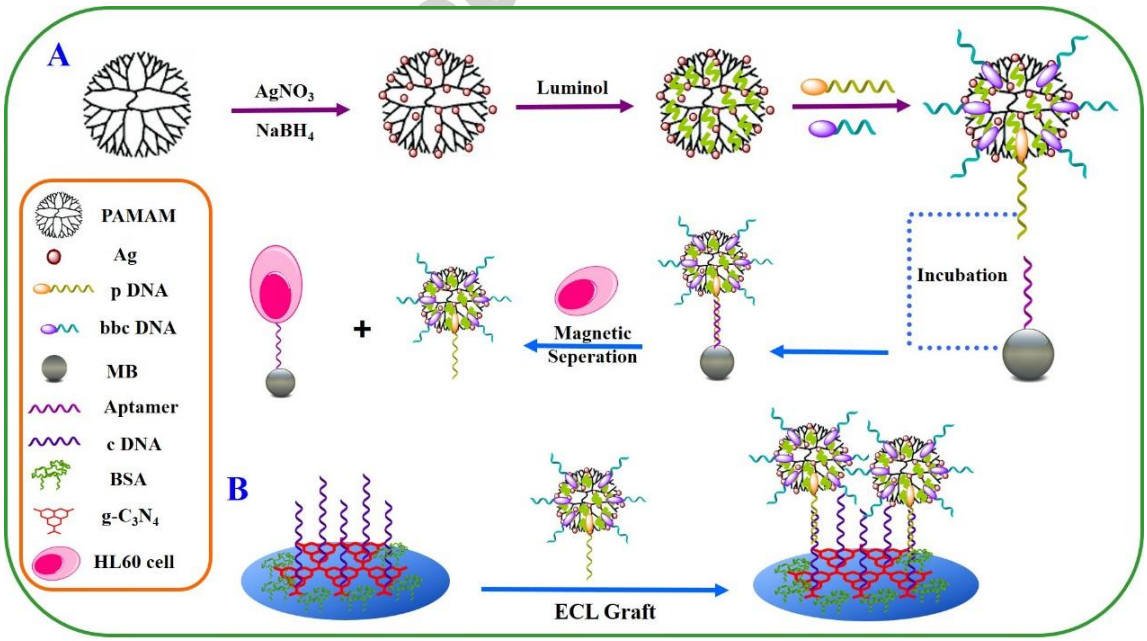

Fig. 1.

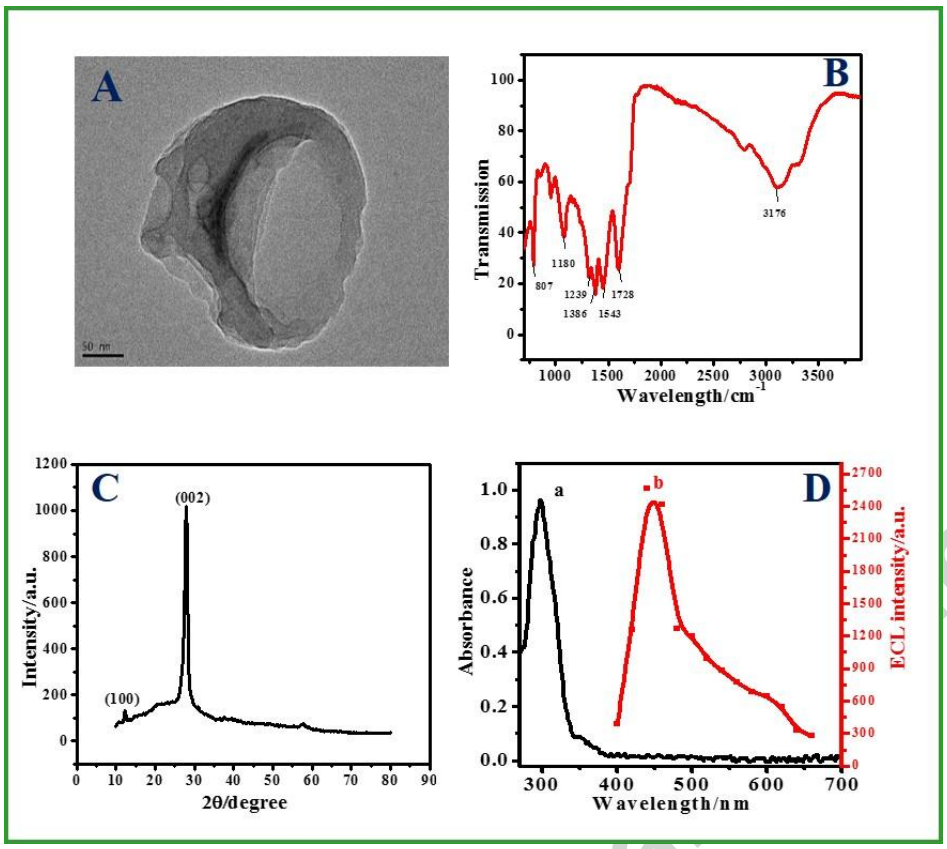
A
50 nm
B
Transmission
Wavelength/cm-1
807
1180
1239
1386
1543
1728
3176
C
Intensity/a.u.
2θ/degree
(100)
(002)
D
Absorbance
ECL intensity/a.u.
Wavelength/nm
a
b

Fig. 2.

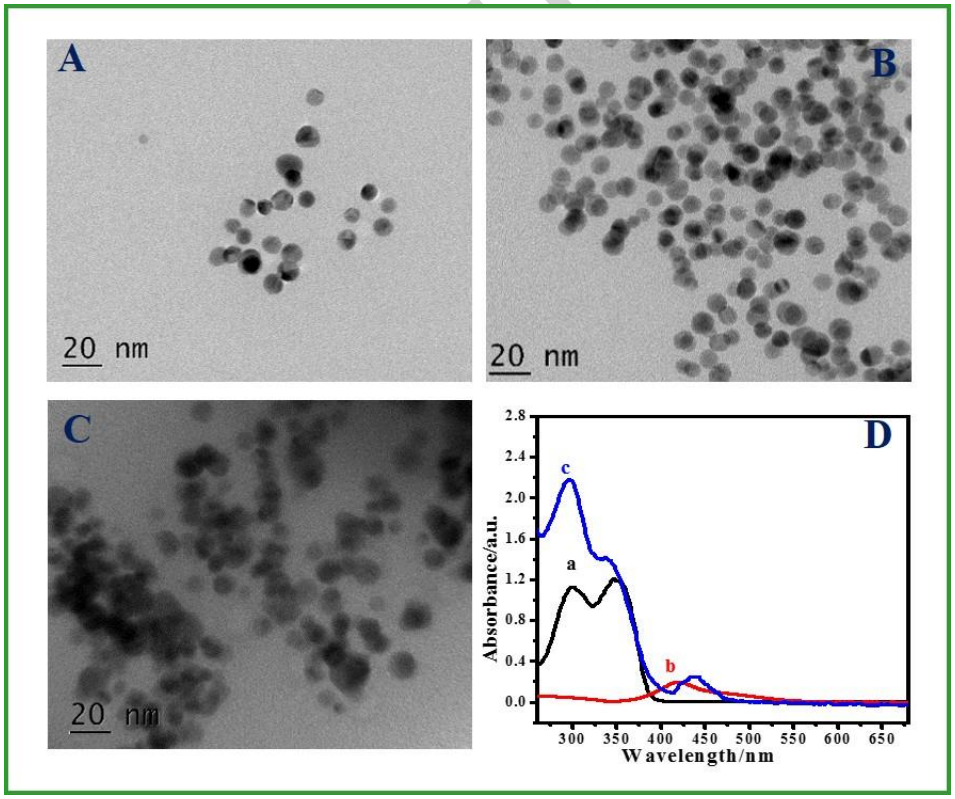
A
20 nm
B
20 nm
C
20 nm
D
Absorbance/a.u.
Wavelength/nm
a
b
c

Fig. 3.

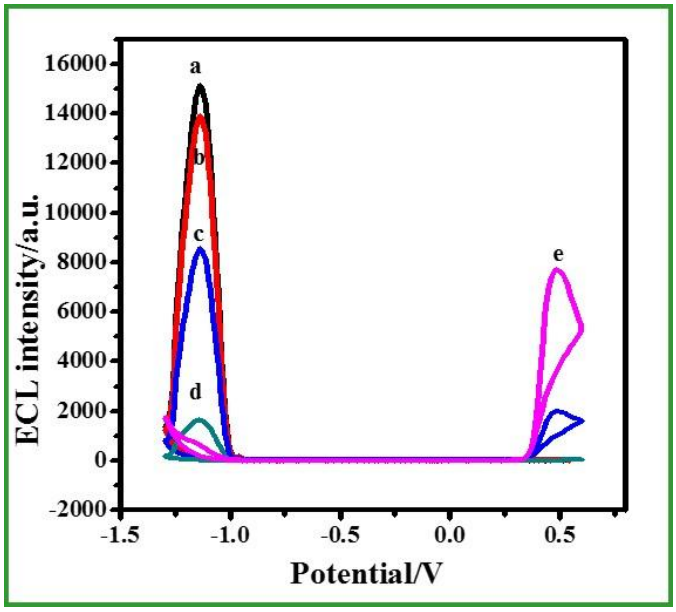

Fig. 4.

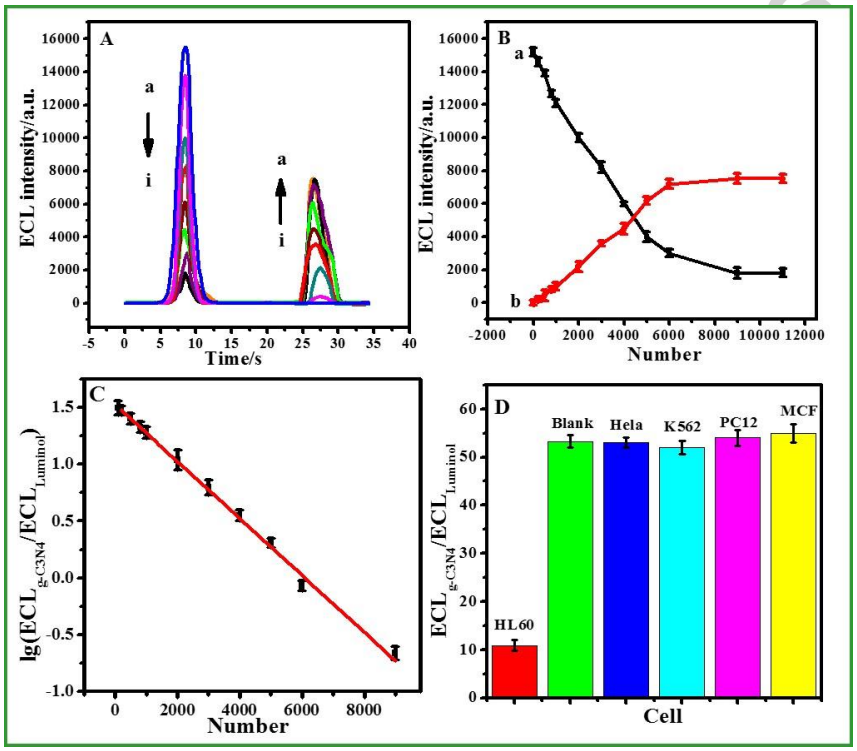

Highlights

>A novel ratiometric ECL biosensor for cancer cells detection was designed.

> g-C_3N_4 nanosheets immobilized on ITO electrode acted as reductive–oxidative ECL emitter.

> Luminol in Ag-PAMAM-luminol biocomposite acted as oxidative−reductive ECL emitter.

> Ag-PAMAM composite not only as the ECL quencher of g-C_3N_4, but also as the carrier for lots of luminol.

>The ECL ratio between both emitters could be controlled by DNA hybridization.